Letters

Thermoplastic Laminate and Cordierite/Indialite Glass-Ceramic Hybrid Package for 15-GHz Operated Antennas

S. Myllymäki, M. Sonkki, *Senior Member, IEEE*, M. Kokkonen, A. Ghavidel, H. Ohsato, and H. Jantunen

***Abstract*— This work describes a novel antenna package, a combination of a four-element array and a lens antenna performing the gain of 13.5 dBi, the bandwidth of 1 GHz and the total efficiency of 72% at 15 GHz. The 2 × 2 elements array antenna was designed and fabricated using square patches with a substrate through vias and a capacitive feeding on the novel dielectric substrate combination: thermoplastic laminate and cordierite/indialite glass-ceramic. The ceramic substrate was selected regarding its impressive dielectric properties such as the relative permittivity of 6.3 and a quality factor Qf 55 400 GHz. The array antenna performed with a reflection coefficient -20 dB over the bandwidth. The cascaded array with an extended hemispherical lens antenna enhanced the gain into the certain direction with narrow beamwidth properties. The packaged antenna is demonstrated for the 5G telecommunication systems especially where low losses, high-temperature resistance, and high-temperature stability are required.**

***Index Terms*— Antenna arrays, ceramic material, lens antennas, thick-film circuit packaging.**

I. Introduction

MOBILE telecommunication systems are being executed and optimized for mmWave frequencies.

The high-end mobile radio and wireless communications systems have increased demands for advanced electronics packages for antenna arrays and the development is moving from the first technology implementations to high yield products.

Earlier known means for electronics packages are circuit housing, it's environmental protection, mechanical support, power supply, signal distribution, and heat conducting structure.

For 5G systems point of view, the system-integration platforms (SiPs) including materials and interconnects are being used for the passive component purposes such as antenna arrays, passive structure components, and feeding networks described in [1] and [5].

SiP packages used in 5G systems typically require or provide several particular technology properties: the integration of passive components with high quality factor, the integration of high gain antenna arrays, electromagnetic compatibility within high-density circuits, wideband interconnections and power integrity, heterogeneous integration of several technologies, and finally high yield in fabrication and sufficient repairability.

High-gain mmWave antenna arrays need low-loss dielectrics, metallization layers, and their feeding/matching networks. Thus, following technical requirements apply to them: small relative dielectric permittivity and low-loss tangents, the quality of conductors, roughness and microstructure, adjustable thickness or permittivity of dielectric layers to optimize the bandwidth of the antenna and temperature stability and resistance for environmental circumstances.

Manuscript received December 15, 2021; revised March 22, 2022; accepted March 23, 2022. Date of publication March 30, 2022; date of current version May 2, 2022. This work was supported by Academy of Finland 6 Genesis Flagship under Grant 318927. Recommended for publication by Associate Editor A. Durgun upon evaluation of reviewers' comments. *(Corresponding author: S. Myllymäki.)*

The authors are with Microelectronics Research Unit, University of Oulu, 90014 Oulu, Finland (e-mail: sami.myllymaki@oulu.fi).

Color versions of one or more figures in this article are available at https://doi.org/10.1109/TCPMT.2022.3163557.

Digital Object Identifier 10.1109/TCPMT.2022.3163557

The proposed heterogeneous integration enables the system to be optimized using different technologies and adjustable system functionality. The integration of radio chips, antenna arrays, and passive components in different layers using different technologies are chosen to optimize the performance of each component without compromising the performance of the other components.

The integration is described also in Smart Electronic System topic, where the structural integration merges layers seamlessly together [6]. Thus, the fabrication of different components in one SiP package by applying several processes and materials end up for high-performance RF system, high yield in the fabrication, and long life-time for the product.

In addition, the specific reliability question raises by the poor efficiency of power amplifiers while they dissipate heat causing a risk for thermo-mechanical issues. Thus, the direct thermal path for the heat should be assured or alternatively heat sinks should be applied. Materials and interconnects in the SiP package must ensure cost-effectiveness via, for example, panel-level packaging, scalability, and reparability due to expensive product's bill of materials (BOM).

Due to previous circumstances, low permittivity, low loss, and high temperature, stabile ceramics are applied on millimeter-wave antenna package in this study.

Recently, microwave and millimeter-wave dielectric ceramics are being developed for wireless communications. Substrates with high quality factor (Qf), low dielectric constant (ε_r), and near-zero temperature coefficient of resonance frequency (τ_f) [7]. They also require other physical properties such as high thermal conductivity and low thermal expansion.

Silicate materials are suitable for millimeter-wave and microwave dielectrics due to low dielectric constant, and the crystal structure consists of silicon tetrahedron SiO_4 with 50% covalency and 45% ionic bonds, and the TiO_6 octahedron provides the highest permittivity value due to the significant rattling factor as the presence of Ti–O ionic bonds, and corundum (Al_2O_3) provides a mid-range permittivity value due to repulsion between Ti–Ti bonds shared in a 2:3 ratio in the octahedron.

Varghese *et al.* [8] reported that indialite/cordierite is one of the silicates reported to have excellent properties and thus being suitable for microwave and millimeter-wave applications.

Indialite/cordierite ($Mg_2Al_4Si_5O_{18}$) +10 wt.% is one of the solid-state synthetic silicates that have good dielectric properties, which has a quality factor Qf = 55 400 GHz, a relative permittivity of 6.3, a temperature coefficient of resonance frequency of (τ_f) of −21 ppm/°C, and a density of 2.6 g/cm^3.

For comparison, $Li_2Mg_2TiO_5$ ceramic has a dielectric permittivity of 13.4, a quality factor of 95 000 GHz (at 11.3 GHz), and a temperature coefficient of resonance frequency of −32.5 ppm/°C [9]. $Li_3Mg_2NbO_6$ ceramic has a dielectric permittivity of 15.8, Qf = 150 000 GHz (9.85 GHz), and $\tau_f = -29$ ppm/°C [10]. However, both of them have higher permittivity and temperature coefficients for ceramic material, thus increasing side-lope problems and remarkably ease the temperature stability issues in the radio design.

In this study, 15-GHz operated 2 × 2 lens antenna array was designed, fabricated, and measured on top of heterogeneous

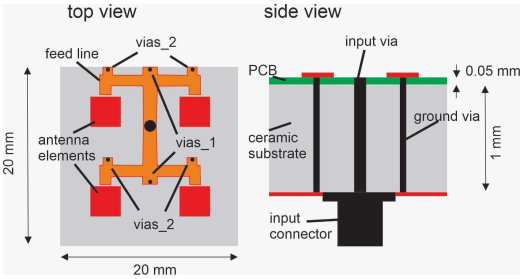

Fig. 1. Schematic views of SiP antenna package. (a) Top view of a 2×2 element antenna printed on a circuit board and the cordierite/indialite glass ceramic substrate. (b) Side view of antenna package.

integrated thin thermoplastic laminates and cordierite/indialite glass ceramic substrates.

The SiP package consists of a ceramic substrate as low-loss material for antennas and at the same time a good choice for further amplifier integration in the package. A hemispherical polymer lens was used to meet sufficient performance values for a 4 × 4 radiator antenna compared to state-of-art antennas at the 15 GHz band; a linear array antenna performed 12.5 dBi gain [11], grid array antenna [12] gain of 12.7 dBi, and efficiency of 66%. Additionally, 15-GHz operated antenna with a directivity of 15 dBi was mentioned in [13].

Lens structure was used on top of the SiP package to meet antenna gain performance, to improve the antenna pattern quality for the main beam and to decrease the power level of sidelobes in the antenna. Over 95% of current antenna lens applications are built either on silicon [14] or polymer materials [15]. Only few applications were realized on other substrates such as flat lens on LTCC ceramic packages [16]. A multilayer substrate-integrated and aperture-coupled AiP antenna performed with 5 dBi gain for a single antenna element and 4-GHz bandwidth at 30 GHz [17].

Silicon lens has good electrical and mechanical match with IC located antennas, whereas polymer lens provides adjustable material properties as well as flexible fabrication methods such as 3-D printing.

Here, polymer material was selected for the SiP package antenna providing also low signal mismatch and low backscattering from the reflective surface.

The lens has several purposes in telecommunications: Lens is used to increase the antenna aperture and thus increase the antenna gain. Lens is used to steer the angular direction of the antenna radiation pattern in terms of antenna location on the lens surface.

In addition, in this letter, lens was designed to improve the yield in the antenna fabrication. Small change in the antenna radiation pattern of SiP package would not be as detrimental cause since the beam is collected and collimated again in the lens. This is one new feature introduced in the letter.

II. Experimental Research

The studied antenna 2 × 2 array was built on thermoplastic laminate, and a ceramic substrate as described in Fig. 1.

Conventional one-side metal-patterned 50-μm-thick laminate (XT/duroid 8000, Rogers Corporation) was utilized to make the antenna pattern on top of the 1-mm-thick cordierite/indialite glass ceramic substrate, where the ground plane was located, and silver (951, Dupont Corporation) printed on the backside of the substrate.

The input antenna port (gold, SMA, Amphenol Corporation) was located on the backside of the SiP package and the signal pin was solder ($Sn_{96.5}/Ag_{3.0}/Cu_{0.5}$) connected through the ceramic substrate to the antenna feed network on the laminate. The laminate and ceramic substrate were attached together by vias and the pin, and

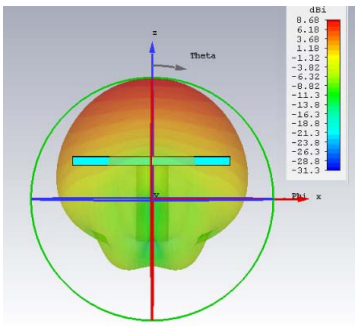

Fig. 2. Simulated antenna radiation pattern seen in the 0° plane in the spherical coordinates (phi0 cut).

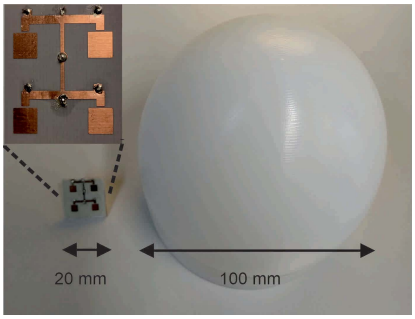

Fig. 3. Photograph of the studied 2 × 2 antenna array and extended hemispherical lens. An antenna array is in operation located behind and in the center of the lens surface.

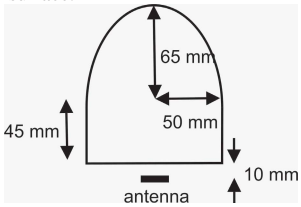

Fig. 4. Schematic of extended hemispherical lens and the antenna array.

no chemical bonding was used. To reach more bandwidth, six metal vias (copper, discrete) were solder connected from the ground plane to the feed network.

The antenna with four rectangular patches were designed above an indialite/cordierite glass ceramics substrate and the feed network was characterized as a phase symmetric impedance matching network for all elements resonating at 15 GHz and generating a summative radiation pattern in perpendicular to the antenna surface.

Beside metal via impact on the bandwidth, capacitive feeding was selected to the feed network enabling *LC*-parameter tuning with enhanced impedance matching of the network. The laminate and the ceramic substrate were used as antenna substrates in the design. A total of six vias were used for balancing the input impedance and the radiation pattern at 15 GHz band.

The antenna simulation with four discrete ports provided the gain of 10.6 dBi. However, the addition of feed network decreased gain by 7 dB. Then the impedance matching was improved by adding vias 1, and beam radiation was optimized by adding vias 2. Finally, the simulated antenna radiation pattern with a maximum directivity of 8.68 dBi and a total efficiency of −1.25 dB (75%) are presented in Fig. 2.

Furthermore, the antenna was equipped with the antenna lens (extended a hemispherical shape, high-density polyethylene permittivity 2.3, tanδ 0.0005) as shown in Figs. 3 and 4.

The designed extension length of the lens was 45 mm, horizontal radius was 50 mm, and vertical radius was 65 mm, and the SiP antenna package was located at 10 mm distance in the center of the lens.

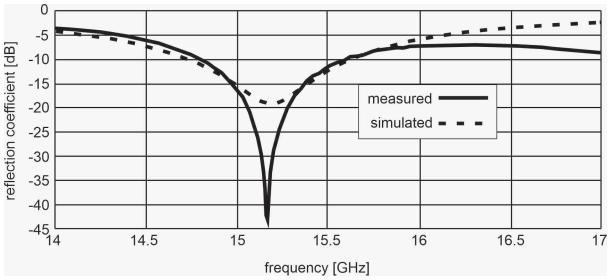

Fig. 5. Simulated and measured impedance matching of lens antenna from 14 to 17 GHz.

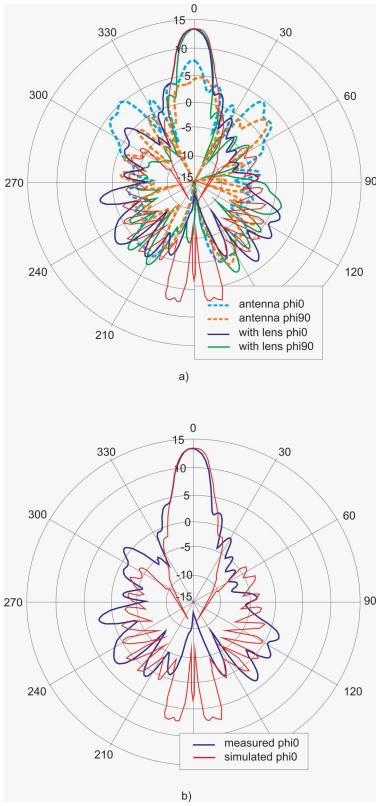

Fig. 6. (a) Measured antenna patterns of antenna with and without lens in the 0° and 90° planes in the spherical coordinates at 15 GHz. (b) Measured and simulated antenna patterns of lens antenna in the 0° plane in the spherical coordinates at 15 GHz.

The lens antenna impedance matching, the radiation patterns, and the efficiency of the antenna were measured with Keysight (N5247B) Microwave Network Analyzer (10 MHz to 67 GHz) and SATIMO StarLab measurement systems capable up to 18 GHz antenna measurements.

Simulated and measured antenna impedance matching are presented in Fig. 5 from 14 to 17 GHz. The matching level was −45 dB at 15.2 with 1 GHz bandwidth (−8 dB), which is very good matching and sufficient bandwidth for the application.

The center resonance frequency versus environmental temperature of the antenna was measured at 20 °C–50 °C range. The resonance frequency decreased only by 0.04%, whereas typical conventional antenna materials such as FR-4, Quartz, polyimide, and Teflon performed over 0.23% at the same temperature range [18].

Antenna radiation patterns were measured with and without lens and presented in Fig. 6(a). Both antenna patterns of 0° and 90° planes in the spherical coordinates (phi0 and phi90) are reported.

The main beam of the antenna in phi0 was well balanced whereas phi90 was a little bit tilted to the clockwise direction. The amplitude of radiation was 4.7 dBi in phi90 and 8.0 dBi in phi0. After installation of the lens, amplitudes of phi90 increased to 13.5 dBi and phi0 to 13.3 dBi. The backside radiation of the antenna package somewhat increased due to the reflection from the lens surface but that characteristic would be reduced by using a larger size reflector or impedance matching layers in further designs.

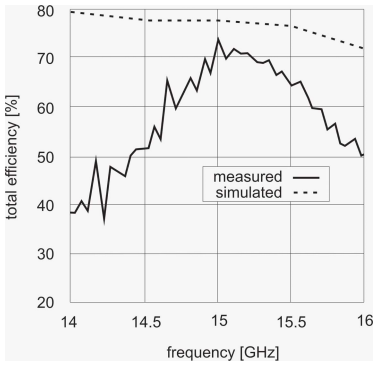

Fig. 7. Simulated and measured total efficiency of antenna from 14 to 16.5 GHz.

TABLE I
COMPARISON OF ANTENNA PERFORMANCES AT 15 GHz

	Element count	Gain [dBi]	Efficiency [%]	Aperture area [mmxmm]	Aperture Height
This work	4	13.5	72	100x100	120 mm
[11]	8	12.5	-	80x10	1 mm
[12]	23	12.7	66	60x50	1.6 mm
[13]	2	15.0	-	-	-
[19]	1	2.5	-	10x20	0.5 mm
[20]	16	18.3	32	106x183	2 mm
[21]	1	5	-	30x29	1.29 mm
[22]	1	12	70	29x29	80 mm
[23]	1	18.5	-	130x130	40 mm

Even though antenna phi0 and phi90 radiation patterns were not complementary for each other, after lens installation they were almost similar. Thus, a change in the antenna radiation pattern of the SiP package would be insignificant after lens installation and the lens decreases the manufacturing variance.

Fig. 6(b) presents a comparison of simulated and measured lens antenna patterns of 0° plane revealing their good correlation. Simulated and measured total efficiencies of the antenna package from 14 to 16 GHz are presented in Fig. 7.

The maximum total efficiency is 72% that is close to the simulated value of 76%. The main physical and electrical parameters of antennas are compared to references in Table I.

Antenna gain of 12.5 dB was measured in [11] and gain of 12.7 dB with 66% efficiency at 15 GHz in [12], emphasizing good antenna efficiency values in this study. X-band-operated lens antennas performed gains of 12 and 18 dB, respectively, in [23] and [24]. Simulated and measured electrical performance values were complementary to each other, and the proposed SiP lens antenna package can be well applied for the 5G telecommunication applications.

III. CONCLUSION

The 2 × 2 element array was fabricated by thermoplastic laminate and cordierite/indialite glass-ceramic, cascaded with an extended lens antenna as whole as a novel solution for the antenna package.

It performed over 1-GHz bandwidth with a −20 dB reflection coefficient (S_{11}), 13.5 dBi gain, and 72% total efficiency. Capacitive feeding and metal via contributed wide bandwidth and very good impedance matching on the presented antenna.

The antenna package can be well utilized for several 5G telecommunication applications. It's best characteristics are low losses, high thermal resistance, high thermal stability, and heat conducting capacity.

REFERENCES

[1] I. Ndip and K.-D. Lang, "Roles and requirements of electronic packaging in 5G," in *Proc. 7th Electron. Syst.-Integr. Technol. Conf. (ESTC)*, Sep. 2018, pp. 1–5, doi: 10.1109/ESTC.2018.8546469.

[2] T. Nishio, "Electronic packaging gears up for 5G mobile race," in *Proc. Int. Conf. Electron. Packag. (ICEP)*, Apr. 2017, pp. 328–332, doi: 10.23919/ICEP.2017.7939388.

[3] M. Tsai *et al.*, "Innovative packaging solutions of 3D double side molding with system in package for IoT and 5G application," in *Proc. IEEE 69th Electron. Compon. Technol. Conf. (ECTC)*, May 2019, pp. 700–706, doi: 10.1109/ECTC.2019.00111.

[4] A. Watanabe *et al.*, "Leading-edge and ultra-thin 3D glass-polymer 5G modules with seamless antenna-to-transceiver signal transmissions," in *Proc. IEEE 68th Electron. Compon. Technol. Conf. (ECTC)*, May 2018, pp. 2026–2031, doi: 10.1109/ECTC.2018.00304.

[5] N. S. Jeong, Y.-C. Ou, A. Tassoudji, J. Dunworth, O. Koymen, and V. Raghavan, "A recent development of antenna-in-package for 5G millimeter-wave applications (invited paper)," in *Proc. IEEE 19th Wireless Microw. Technol. Conf. (WAMICON)*, Apr. 2018, pp. 1–3, doi: 10.1109/WAMICON.2018.8363905.

[6] L.-R. Zheng, H. Tenhunen, and Z. Zou, *Smart Electronic Systems: Heterogeneous Integration of Silicon and Printed Electronics*, Sep. 2018, p. 296.

[7] H. Ohsato, J.-S. Kim, A.-Y. Kim, C.-I. Cheon, and K.-W. Chae, "Millimeter-wave dielectric properties of cordierite/indialite glass ceramics," *Jpn. J. Appl. Phys.*, vol. 50, no. 9, Sep. 2011, Art. no. 09NF01.

[8] J. Varghese, T. Vahera, H. Ohsato, M. Iwata, and H. Jantunen, "Novel low-temperature sintering ceramic substrate based on indialite/cordierite glass ceramics," *Jpn. J. Appl. Phys.*, vol. 56, no. 10S, Oct. 2017, Art. no. 10PE01.

[9] C. Li, H. Xiang, and C. Yin, "Ultra-low loss microwave dielectric ceramic $Li_2Mg_2TiO_5$ and low-temperature firing via B_2O_3 addition," *J. Electron. Mater.*, vol. 47, pp. 6383–6389, Nov. 2018, doi: 10.1007/s11664-018-6595-9.

[10] G. Wang *et al.*, "Investigation and characterization on crystal structure and enhanced microwave dielectric properties of non-stoichiometric Li3+xMg2NbO6 ceramics," *Ceram. Int.*, vol. 44, no. 16, pp. 20539–20544, Nov. 2018, doi: 10.1016/j.ceramint.2018.08.051.

[11] B. Xu *et al.*, "Power density measurements at 15 GHz for RF EMF compliance assessments of 5G user equipment," *IEEE Trans. Antennas Propag.*, vol. 65, no. 12, pp. 6584–6595, Dec. 2017, doi: 10.1109/TAP.2017.2712792.

[12] M. S. Yahya and S. K. A. Rahim, "15 GHz grid array antenna for 5G mobile communications system," *Microw. Opt. Technol. Lett.*, vol. 58, no. 12, pp. 2977–2980, Dec. 2016, doi: 10.1002/mop.30190.

[13] P. Okvist, H. Asplund, A. Simonsson, B. Halvarsson, J. Medbo, and N. Seifi, "15 GHz propagation properties assessed with 5G radio access prototype," in *Proc. IEEE 26th Annu. Int. Symp. Pers., Indoor, Mobile Radio Commun. (PIMRC)*, Aug. 2015, pp. 2220–2224, doi: 10.1109/PIMRC.2015.7343666.

[14] M. Alonso-Delpino, C. Jung-Kubiak, T. Reck, N. Llombart, and G. Chattopadhyay, "Beam scanning of silicon lens antennas using integrated piezomotors at submillimeter wavelengths," *IEEE Trans. THz Sci. Technol.*, vol. 9, no. 1, pp. 47–54, Jan. 2019, doi: 10.1109/TTHZ.2018.2881930.

[15] Y.-X. Zhang, Y.-C. Jiao, and S.-B. Liu, "3-D-printed comb mushroom-like dielectric lens for stable gain enhancement of printed log-periodic dipole array," *IEEE Trans. Antennas Propag.*, vol. 17, no. 11, pp. 2099–2103, Nov. 2018.

[16] M. Imbert, J. Romeu, M. Baquero-Escudero, M. Martinez-Ingles, J. Molina-Garcia-Pardo, and L. Jofre, "Assessment of LTCC-based dielectric flat lens antennas and switched-beam arrays for future 5G millimeter-wave communication systems," *IEEE Trans. Antennas Propag.*, vol. 65, no. 12, pp. 6453–6473, Dec. 2017.

[17] D. Liu, X. Gu, C. W. Baks, and A. Valdes-Garcia, "An aperture-coupled dual-polarized stacked patch antenna for multi-layer organic package integration," in *Proc. IEEE Int. Symp. Antennas Propag. USNC-URSI Radio Sci. Meeting*, Jul. 2019, pp. 277–278, doi: 10.1109/APUSNCURSINRSM.2019.8888312.

[18] S. Maurya, R. L. Yadava, and R. K. Yadav, "Effect of temperature variation on microstrip patch antenna and temperature compensation technique," *Int. J. Wireless Commun. Mobile Comput.*, vol. 1, no. 1, pp. 35–40, Jan. 2013, doi: 10.11648/j.wcmc.20130101.16.

[19] A. Sharma, K. Khare, and S. C. Shrirastava, "Dielectric resonator antenna for X band microwave application," *Int. J. Adv. Res. Elect., Electron. Instrum. Eng.*, vol. 2, no. 6, pp. 2247–2252, Jun. 2013.

[20] S.-H. Hsu, Y.-J. Ren, and K. Chang, "A dual-polarized planar-array antenna for S-band and X-band airborne applications," *IEEE Antennas Propag. Mag.*, vol. 51, no. 4, pp. 70–78, Aug. 2009.

[21] A. A. Eldek, A. Z. Elsherbeni, and C. E. Smith, "Wide-band modified printed bow-tie antenna with single and dual polarization for C- and X-band applications," *IEEE Trans. Antennas Propag.*, vol. 53, no. 9, pp. 3067–3072, Sep. 2005.

[22] R. J. Bauerle, R. Schrimpf, E. Gyorko, and J. Henderson, "The use of a dielectric lens to improve the efficiency of a dual-polarized quad-ridge horn from 5 to 15 GHz," *IEEE Trans. Antennas Propag.*, vol. 57, no. 6, pp. 1822–1825, Jun. 2009, doi: 10.1109/TAP.2009.2019929.

[23] H. Li, G. Wang, H.-X. Xu, T. Cai, and J. Liang, "X-band phase-gradient metasurface for high-gain lens antenna application," *IEEE Trans. Antennas Propag.*, vol. 63, no. 11, pp. 5144–5149, Nov. 2015, doi: 10.1109/TAP.2015.2475628.